

Double Beta Decay of ^{150}Nd

R. Arnold¹, C. Augier², J. Baker³, A.S. Barabash⁴, M. Bongrand², G. Broudin², V. Brudanin⁶, A.J. Caffrey³,
 V. Egorov⁶, A.I. Etienvre², N. Fatemi-Ghomi⁷, F. Hubert⁵, Ph. Hubert⁵, J. Jerie⁸, S. Jullian²,
 S. King⁹, O. Kochetov⁶, S.I. Konovalov⁴, V. Kovalenko⁶, D. Lalanne², F. Leccia⁵, Y. Lemièrè¹⁰,
 C. Longuemare¹⁰, G. Lutter⁵, Ch. Marquet⁵, F. Mauger¹⁰, A. Nachab⁵, H. Ohsumi¹¹, F. Perrot⁵,
 F. Piquemal⁵, J.L. Reyss¹², J.S. Ricol⁵, R. Saakyan⁹, X. Sarazin², L. Simard², F. Šimkovic¹³, Yu. Shitov⁶,
 A. Smolnikov⁶, S. Söldner-Rembold⁷, I. Štekl⁸, J. Suhonen, C.S. Sutton, G. Szklarz², J. Thomas⁹,
 V. Timkin⁶, V. Tretyak⁶, V. Umatov⁴, L. Vála⁸, I. Vanyushin⁴, V. Vasiliev⁹, V. Vorobel¹⁵, and Ts. Vylov⁶

(The NEMO 3 Collaboration)

¹*IPHC, IN2P3-CNRS et Université Louis Pasteur, F-67037 Strasbourg, France*

²*LAL, IN2P3-CNRS et Université Paris-Sud, F-91405 Orsay, France*

³*INEEL, Idaho Falls, ID83415, USA*

⁴*Institute of Theoretical and Experimental Physics, 117259 Moscow, Russia*

⁵*CENBG, IN2P3-CNRS et Université Bordeaux I, F-33170 Gradignan, France*

⁶*Joint Institute for Nuclear Research, 141980 Dubna, Russia*

⁷*University of Manchester, M13 9PL Manchester, United Kingdom*

⁸*IEAP, Czech Technical University in Prague, CZ-12800 Prague, Czech Republic*

⁹*University College London, WC1E 6BT London, United Kingdom*

¹⁰*LPC, IN2P3-CNRS et Université de Caen, F-14032 Caen, France*

¹¹*Saga University, Saga 840-8502, Japan*

¹²*LSCE, CNRS, F-91190 Gif-sur-Yvette, France*

¹³*FMFI, Comenius University, SK-842 48 Bratislava, Slovakia*

¹⁴*Jyväskylä University, 40351 Jyväskylä, Finland*

¹⁵*MHC, South Hadley, Massachusetts, MA01075, USA and*

¹⁶*Charles University, Prague, Czech Republic*

(Dated: July 2, 2008)

The half-life for double beta decay of ^{150}Nd has been measured by the NEMO 3 experiment at the Modane Underground Laboratory. Using 939 days of data recorded with 37 g of ^{150}Nd the half-life for $2\nu\beta\beta$ decay is measured to be $T_{1/2}^{2\nu} = (9.20_{-0.22}^{+0.25}(\text{stat.}) \pm 0.62(\text{syst.})) \times 10^{18}$ years. The limit on the half-life for neutrino-less double beta decay is found to be $T_{1/2}^{0\nu} > 1.45 \times 10^{22}$ years at 90% Confidence Level. This translates into a limit on the effective Majorana neutrino mass of $\langle m_\nu \rangle < 1.9 - 2.7$ eV.

PACS numbers: 14.60.pq, 23.40.-s

Neutrinoless double beta decay ($0\nu\beta\beta$) violates lepton number and is therefore a direct probe for physics beyond the standard model (SM). The observation of neutrinoless double beta decay would prove that neutrinos are Majorana particles and give the absolute mass scale of the neutrinos. Neodymium-150 (^{150}Nd) has one of the highest $Q_{\beta\beta}$ values for double beta decay, $Q_{\beta\beta} = 3.367$ MeV [1]. This value of $Q_{\beta\beta}$ lies above the typical energies for many background sources. This and the large phase space factor make ^{150}Nd a very interesting candidate for SuperNEMO [3], the next generation double beta decay experiment based on the NEMO 3 concept, and SNO++ [4]. The half-life of $2\nu\beta\beta$ decay of ^{150}Nd has previously been measured using a Time Projection Chamber [5, 10]. The single neodymium composite source foil in NEMO 3 is composed of 40.63 g enriched Nd_2O_3 , corresponding to a ^{150}Nd mass of 37.0 ± 0.1 g [2].

The NEMO 3 experiment has been taking data since 2003 in the Modane Underground Laboratory (LSM) located in the Frejus tunnel at a depth of 4800 m water equivalent. The experiment has a cylindrical shape with 20 sectors that contain different isotopes in the form of thin foils with a total surface of about 20 m². In addition to ~ 7 kg of ^{100}Mo and ~ 1 kg of ^{82}Se , the detector contains smaller amounts of other isotopes. On each side of the foils is a ~ 50 cm wide tracking volume comprising a total of 6180 drift cells operated in Geiger mode with a typical vertex resolution of 5 mm and 8 mm in the coordinates transverse and perpendicular to the foil, respectively. The drift gas is helium with admixtures of 4% ethyl alcohol, 1% argon and 0.1% water. A 25 Gauss magnetic field created by a solenoid provides charge identification. The calorimeter consists of 1940 plastic scintillators coupled to low radioactivity photomultipliers. For

1 MeV electrons the energy resolution (FWHM) ranges from 14.1% to 17.7% and the timing resolution is 250 ps. A cylindrical coordinate system is used (r, z) with the z axis pointing upwards.

The data set used in this letter has been recorded between February 2003 and December 2006, corresponding to 939 days of data taking.

The background sources are divided into two categories, depending on their origin. Background events originating from the radioactive impurities in the source foils are called internal background. β^- emitters can produce $\beta\beta$ -like events through three mechanisms: β decay accompanied by an electron conversion; Møller scattering of a β decay electron, and β decay to an excited state followed by Compton scattering of the de-excitation photon. Another internal source of background is ^{207}Bi , most likely due to a contamination of the ^{150}Nd source foil during production. This isotope decays to excited ^{207}Pb through electron capture (EC) and ^{207}Pb subsequently emits two electrons via electron conversion.

The second source of background is called external and is caused by electrons or photons anywhere outside the source foils [11]. The main source of the external background is due to radon that is outgassed from the rock walls surrounding the detector. Radon decays to ^{214}Pb via two α decays and subsequently to ^{214}Bi via β^- decay. The decay of ^{214}Bi to ^{214}Po is generally accompanied by one electron and several photons, which can mimic a $\beta\beta$ event through conversions. A radon purification facility was installed about half-way through the data taking period presented in this Letter. Other external background sources are found to be small.

Background events are generated using a GEANT-based simulation [13] of the detector. All Monte Carlo events are processed by the same reconstruction programs as the data. The activities are determined using high purity germanium (HPGe) measurements and using control channels.

In the $e\gamma$ channel, ^{207}Pb from the ^{207}Bi decays via the emission of an electron and a photon from the strongly-converted energy transition in excited ^{207}Pb . ^{152}Eu decays into excited ^{152}Gd through β decay which de-excites into the ground state via photon emission. The $e\gamma$ events are selected by requiring that exactly one negatively charged track with a track length greater than 50 cm is found in the sector containing the ^{150}Nd foil. The track must be associated with an isolated scintillator hit with energy greater than 0.2 MeV. The track must originate from the ^{150}Nd foil and must have a hit in the first layer of the Geiger cells. The scintillator measurement of the time-of-flight of the electron candidates has to be consistent with the hypothesis that the event originates from the source foil. The photon is identified by requiring that there is a second scintillator hit with energy greater than 0.2 MeV and that the energy sum of the all other clusters not associated to the electron or the photon is less than

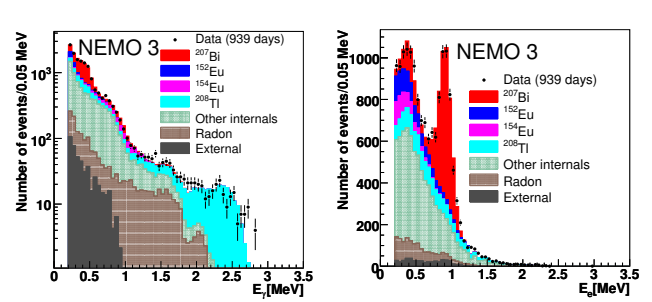


FIG. 1: Energy distributions of the a) photon and b) electron energy in $e\gamma$ events. The data are compared to the sum of the background expectation. All uncertainties are statistical.

0.15 MeV. The opening angle between the electron and the photon is required to be $\cos\theta < 0.9$.

To obtain the background normalisation for ^{207}Bi and ^{152}Eu , these background contributions are fitted to spectra of the photon energies E_γ and the electron energies E_e shown in Figure 1. The contributions from other background sources are fixed in the fit. The ^{208}Ac contribution is taken from the ^{208}Tl component in the high energy tail of the E_γ distribution since ^{208}Tl originates from ^{208}Ac decays. The external, the radon-induced and ^{214}Bi background have been measured independently [11].

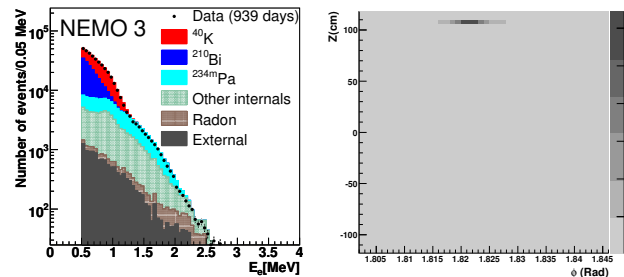


FIG. 2: a) Distribution of the electron energy in single electron events. The data are compared to the sum of the background expectation. b) Distribution of the event vertices in the ^{150}Nd source foil for single electron events.

The isotopes ^{234m}Pa and ^{40}K undergo β decay. Their activities are therefore measured by selecting single electron events. The same selection for the track was applied as in the $e\gamma$ channel, apart from an additional requirement $E_e > 0.5$ MeV. The ^{234m}Pa and ^{40}K contributions are obtained from a fit to the E_e distributions. The ^{210}Bi contribution and the external background are taken from independent measurements [11]. The ^{207}Bi component has been measured in the $e\gamma$ channel and the ^{212}Bi component is normalised with respect to the measurement of its decay product ^{208}Tl . The E_e distribution with the fitted ^{234m}Pa and ^{40}K contributions is shown in Figure 2a. The distribution of the event vertices, defined by

the tracks intersection with the source foil, in the single electron events is shown in Figure 2 b. In the distribution, there is clearly identified region of high activity which is removed in the analysis. This region is consistent with ^{234m}Pa contamination. The activities used in the analysis are measured after the removal of this area.

Due to the resolution of the tracking detector, events from neighboring source foils (^{48}Ca , ^{96}Zr , ^{100}Mo) can be reconstructed as originating from the ^{150}Nd foil. The total number of background events from neighboring foils is estimated to be 130 ± 13 from MC simulations. where the uncertainty is mainly due to the uncertainty on the half-life of these isotopes.

Background	A (mBq/kg)	N_{bg}	N_{bg} $E > 2.5$ MeV
^{152}Eu	54 ± 6	37 ± 4	0
^{208}Tl	10.05 ± 2	47.21 ± 9.3	4 ± 1
^{228}Ac	27.9 ± 5.6	53.1 ± 10.6	0
^{212}Bi	27.9 ± 5.6	33.6 ± 6.7	0
^{207}Bi	231 ± 10	143 ± 6	0
^{214}Bi	3.3 ± 0.8	23 ± 6	0.43 ± 0.11
^{40}K	213 ± 10	67.9 ± 3.19	0
^{234m}Pa	47 ± 2	146.5 ± 6.2	0
^{210}Bi	N.A.	23 ± 1	0
External and Radon	N.A.	56 ± 8	1.0 ± 0.1
Neighboring foils	N.A.	130 ± 13	0.10 ± 0.01
sum		760.31 ± 23.45	

TABLE I: Summary of the measured background activities and the expected number of background events in the data set.

The $2\nu\beta\beta$ events are selected by requiring two tracks with a curvature consistent with a negative charge. Each track has to be matched to a separate energy deposit in the calorimeter of greater than 0.2 MeV. The z component of the distance between the intersections of each track with the plane of the foil should be less than 4 cm and the transverse component less than 2 cm. Both tracks must originate from the first layer of the Geiger cells. The scintillator measurement of the time-of-flight (TOF) for both electron candidates must be consistent with the hypothesis that the event originates from the source foil. After this selection 2828 events remain.

The distributions of the energy sum of the two electrons and the opening angle between them are shown in Figure 3. The data are in good agreement with the sum of the background and the $2\nu\beta\beta$ signal distributions. We therefore use the data sample to measure the $2\nu\beta\beta$ half-life, $T_{1/2}^{2\nu}$, of ^{150}Nd . The efficiency of the $2\nu\beta\beta$ event selection is 7.2%. After background subtraction we obtain

$$T_{1/2}^{2\nu} = (9.20_{-0.22}^{+0.25}(\text{stat.}) \pm 0.62(\text{syst.})) \times 10^{18} \text{ y.} \quad (1)$$

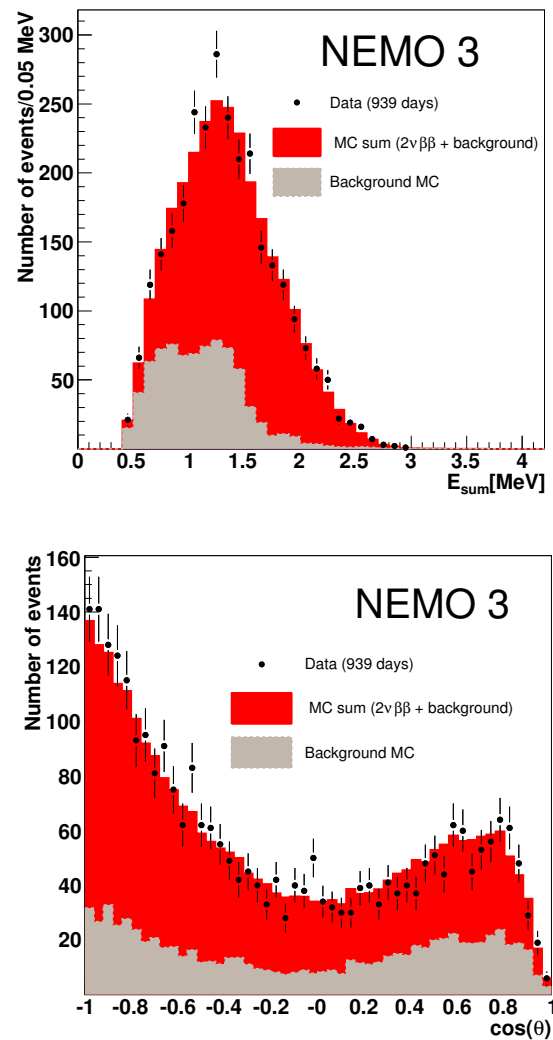


FIG. 3: Distributions of a) the energy sum of the two electrons, E_{sum} , and b) the angle between the two electrons, $\cos \theta$, for data compared to the sum of the background and $2\nu\beta\beta$ signal expectations.

The systematic on the background is 2.7%. This includes the uncertainty on the background from the errors of the background fit and measurement of activity of ^{208}Tl using two different decay channels. The uncertainty on the tracking efficiency is 5% [12]. Varying the TOF requirement leads to a 1% uncertainty. The uncertain 3% from the position of the ^{150}Nd foil in the detector.

Since no excess is observed in the E_{sum} distribution, a limit is set on the half-life for neutrinoless double beta decay $T_{1/2}^{0\nu}$ using the CL_s method [14]. To maximise sensitivity the full E_{sum} distribution in the range $E_{sum} > 2.5$ MeV is used in the limit calculation. The limits are calculated by utilizing a likelihood-fitter [15] that uses a log-likelihood ratio (LLR) test statistic method.

Two hypotheses are defined, the signal-plus-background hypothesis and the background-only hypothesis. The LLR distributions are populated using Poisson simulations of the two hypotheses. Systematic uncertainties are treated as uncertainties on the expected numbers of events and are folded into the signal and background expectations via a Gaussian distribution. The value of the confidence level, CL_s , is defined as $CL_s = CL_{s+b}/CL_b$, where CL_{s+b} and CL_b are the confidence levels in the signal-plus-background and background only hypotheses, respectively. The median expected and observed limits are calculated by scaling the signal until CL_s reaches 90%.

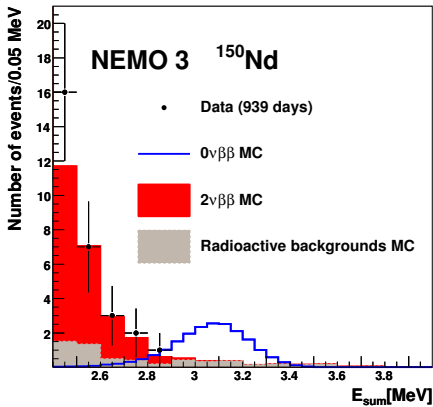


FIG. 4: Distribution of the energy sum of the two electrons, E_{sum} , for $E_{sum} > 2.5$ MeV for data compared to the total background, consisting of internal and external background and the $2\nu\beta\beta$ expectation. A MC simulation of a $0\nu\beta\beta$ signal with a half-life of 1.45×10^{22} years is also shown. All uncertainties are statistical.

The total efficiency for $0\nu\beta\beta$ events after applying all selections is $(19 \pm 1)\%$. The uncertainties on the efficiency of the signal and the background are assumed to be fully correlated. The measured $T_{1/2}^{2\nu}$ and its statistical uncertainty determined for $E_{sum} < 2.5$ MeV are used to normalize the $2\nu\beta\beta$ events. The E_{sum} distribution for $E_{sum} > 2.5$ MeV is shown in Figure 4 for data compared to the total background, which consists of internal and external background and the $2\nu\beta\beta$ expectation. A MC simulation of a $0\nu\beta\beta$ signal is also shown. The limit on

the half-life is $T_{1/2}^{0\nu} > 1.45 \times 10^{22}$ years at 90% Confidence Level (CL). Discuss NME here. The half-life limit translates into a limit on the effective Majorana neutrino mass in the range $\langle m_\nu \rangle < 1.9 - 2.7$ eV.

Limits on other modes of double beta decay is shown in table II.

In summary, we have presented the most precise measurement of the half-life of double beta decay of ^{150}Nd to date, yielding a value of $T_{1/2}^{2\nu} = (9.20^{+0.25}_{-0.22}(\text{stat.}) \pm 0.62(\text{syst.})) \times 10^{18}$ years. This value is slightly more

Mode ($T_{1/2} \times 10^{21}$)	0ν			Majoron			
	$0_1^+(RC)$	$0_1^+(MM)$	$2_1^+(RC)$	n=1	n=2	n=3	n=7
This work	> 12.7	> 7.56	> 0.91[8]	> 1.55	> 1	> 0.3	> 0.1
Previous limits	> 1.1[6]	> 0.15[7]	> 0.91[8]	> 0.28[9]			

TABLE II: Summary of the limits on different modes of double beta decay, for comparison the previous world's best limits are illustrated.

than two standard deviations higher than the previously measured value $T_{1/2}^{2\nu} = (6.75^{+0.37}_{-0.42}(\text{stat.}) \pm 0.68(\text{syst.})) \times 10^{18}$ years [10]. We have also derived limits on different modes of neutrino-less double beta decay based on the measured distribution of the energy sum of the two electrons.

[1] reference needed
[2] TDR reference
[3] SuperNEMO reference
[4] SNO reference
[5] V. Artemiev *et al.*, Phys. Lett. B. **345**, 564 (1995).
[6] A.A. Klimenko *et al.*, Nucl. Instr. Meth. **17**, 445 (1986)
[7] A.A. Klimenko *et al.*, Czech. J. Phys. **52**, 589 (2002)
[8] C. Arpesella *et al.*, Nucl. Phys. B. **70**, 249 (1999)
[9] A. De Silva *et al.* Phys. Rev. C **56**, 2451 (1997)
[10] A. De Silva *et al.*, reference.
[11] R. Arnold *et al.*, to be submitted.
[12] Mo excited state pape
[13] GEANT reference:
R. Brun and F. Carminati, CERN Program Library Long Writup W5013, 1993 (unpublished).
[14] CLS reference
[15] W. Fisher, FERMILAB-TM-2386-E (2007). T. Junk, Nucl. Instrum. Methods A **434**, 435 (1999).